# The impact of mixtures of xylose and glucose on the microbial diversity and fermentative metabolism of sequencing-batch or continuous enrichment cultures

Rombouts, Julius L.; Mos, Galvin; Weissbrodt, David G.; Kleerebezem, Robbert; Van Loosdrecht, Mark C.M.

**DOI**
10.1093/femsec/fiz112

**Publication date**
2019

**Document Version**
Accepted author manuscript

**Published in**
FEMS Microbiology Ecology

Post-print of an original research article published in *FEMS Microbiology Ecology*

# The impact of mixtures of xylose and glucose on the microbial diversity and fermentative metabolism of sequencing-batch or continuous enrichment cultures

Keywords: sequencing batch reactor – chemostat – carbon catabolite repression - microbial selection – mixed substrates

Julius L. Rombouts*, Galvin Mos, David G. Weissbrodt[§], Robbert Kleerebezem[§] and Mark C.M. Van Loosdrecht[§]

Delft University of technology, Department of Biotechnology, Van der Maasweg 9, 2629 HZ Delft, the Netherlands.

* Corresponding author, julesrombouts@gmail.com, +316 15654428

[§] Shared senior authorship.

## Abstract

Efficient industrial fermentation of lignocellulosic waste containing a large part of glucose and xylose is desirable to implement a circular economy. Mixed culture biotechnologies can aid to realise this goal. The effect of feeding equivalent substrates to a microbial community, such a xylose and glucose, is not well understood in terms of number of dominant species and how these species compete for substrate. We compared the metabolism and microbial community structure in a continuous-flow stirred tank reactor (CSTR) and a sequencing batch reactor (SBR) fed with a mixture of xylose and glucose, inoculated with bovine rumen at pH 8, 30°C and a hydraulic retention time of 8 h. We hypothesised that a CSTR will select for generalist species, taking up both substrates. We used 16S rRNA gene sequencing and fluorescent *in situ* hybridisation (FISH) to accurately determine the microbial community structures. Both enrichments were stoichiometrically and kinetically characterised. The CSTR enrichment culture was dominated by *Clostridium intestinale* (91%±2%).The SBR showed an abundance of *Enterobacteriaceae* (75%±8%), dominated by *Citrobacter freundii* and a minor fraction of *Raoultella ornithinolytica*. *Citrobacter freundii* ferments xylose and glucose in a non-diauxic fashion. Clearly, a non-diauxic generalist outcompetes specialists and diauxic generalists in SBR environments.


## Introduction

Glucose and xylose are the two most abundant monomers found in lignocellulosic waste streams (Anwar, Gulfraz and Irshad 2014). Fermentation of these two carbohydrates to valuable compounds such as volatile fatty acids (VFAs), lactic acid, hydrogen or ethanol can enable new biobased processes to be developed (Guo *et al.* 2010; Dionisi *et al.* 2015; Kleerebezem *et al.* 2015). Enrichment culturing offers the potential to apply selective conditions to direct a process towards a certain product, *e.g.* butyrate in carbohydrate fermentation (Kleerebezem and van Loosdrecht 2007), poly-β-hydroxyalkanoates in an

aerobic feast-famine process (Johnson *et al.* 2009) or medium chain fatty acids from volatile fatty acids and an electron donor like ethanol or lactate (Steinbusch *et al.* 2011). Enrichment cultures select for specific microorganisms based on competition for a growth rate limiting substrate (Beijerinck 1901). Most fermentative enrichment studies have been performed using a continuous-flow stirred tank reactor (CSTR) setup (Fang and Liu 2002; Temudo, Kleerebezem and van Loosdrecht 2007; Rafrafi *et al.* 2013). A CSTR is a system where the fermentable substrate is continuously available at a low concentration. This is similar to anaerobic digestion of lignocellulosic waste. The hydrolysis of the macromolecular substrate, *e.g.* cellulose, is the rate-limiting step in the fermentation leading to the hydrolysed monomer substrate, *e.g.* glucose to be continuously available in low residual concentrations (Noike *et al.* 1985; Kleerebezem *et al.* 2015).

In a CSTR, Monod kinetics describe the relationship between the residual substrate concentration ($C_s$), the maximum biomass specific growth rate ($\mu^{max}$), and the affinity constant for the substrate ($K_s$):

$$\mu = \mu^{max} \cdot \frac{C_s}{C_s + K_s} \qquad (1)$$

Since the biomass specific growth rates (μ) of microbial populations in a CSTR environment is set by the dilution rate (D) of the reactor, $C_s$ is a function of the dilution rate and the affinity properties ($\mu^{max}\ K_s^{-1}$) of the microorganisms. The microorganism with the highest affinity for the substrate is expected to dominate the enrichment culture (Hansen and Hubbell 1980), as is shown for two competing yeast species (Postma *et al.* 1989).

In a previous study we have demonstrated this effect. In a CSTR enrichment culture limited with glucose we indeed observed one species dominating (>90%) the population. For xylose we however observed a community with at least three dominant species, indicating other mechanisms besides direct substrate competition are complicating the microbial community structure (Rombouts *et al.* 2019).

Equivalent substrates are compounds which are both used in metabolism in a similar fashion. For example anabolic nitrogen sources or catabolic electron acceptors or donors, or both, in the case of fermentation (Kuenen 2015). When mixing two equivalent substrates, like glucose and xylose, the Monod kinetics model is extended. A simple mathematical view on mixed-substrate kinetics is obtained by summing the individual Monod kinetics as proposed by Bell (1980):

$$\mu = {\mu_1}^{max} \cdot \frac{C_{s,1}}{C_{s,1}+K_{s,1}} + {\mu_2}^{max} \cdot \frac{C_{s,2}}{C_{s,2}+K_{s,2}} \quad (2)$$

This simple model does not normalise for substrate concentrations or ratios, which can improve the modelling of mixtures of carbon (Lendenmann and Egli 1998), but is sufficient to demonstrate the advantage of a generalist over a specialist microorganism.

Two types of microbial species can compete in a mixed-culture CSTR, a specialist taking up only one substrate and a generalist, taking up both substrates simultaneously. If we assume the generalist and specialist species possess similar kinetic properties on xylose and glucose ($\mu^{max}$ $K_s^{-1}$), then the generalist, by converting both xylose and glucose simultaneously, can lower the residual concentration of xylose and glucose beyond the capacity of the specialist species, resulting in wash-out of the specialists (Kuenen 2015). This effect has been demonstrated in pure culture competition experiments with two specialists and one generalist (Gottschal, de Vries and Kuenen 1979; Kuenen 1983). We thus expect a generalist species to dominate the CSTR environment.

The sequencing batch reactor (SBR) environment offers the opportunity to select for a microbial community based on the maximum biomass-specific growth rate ($\mu^{max}$). When feeding a mixture of xylose and glucose to a microbial community at high concentrations, carbon catabolite repression (CCR) or diauxic behaviour is expected favoured for substrate uptake, where glucose is first taken up prior to xylose. The preference for glucose is mediated through a cyclic AMP (cAMP) regulated pathway in *E.coli,* therefore glucose is preferably metabolised (Deutscher 2008). CCR is an abundant mechanism amongst

heterotrophic bacteria (Görke and Stülke 2008). It has been demonstrated that in a batch environment, specialist species will outcompete a diauxic generalist species (Gottschal, de Vries and Kuenen 1979). This theory has been confirmed for an enrichment of microorganisms accumulating PHA on a mixture of acetate and lactate, where *Plasticicumulans acidivorans* was identified as acetate specialist and *Thauera selenatis* as lactate specialist (Jiang *et al.* 2011). Thus, we believe a competitive CCR-type species will take up the glucose, leaving a niche for a sole xylose specialist to take up the xylose. In other words, we expect that in an SBR enrichment culture fed with a mixture of glucose and xylose, two specialist species will be enriched in the microbial community.

The fed-batch environment is typically used in industrial fermentations using pure cultures to convert sugars to a desired product (Meyer, Minas and Schmidhalter 2017). When using a mixture of substrates in a fed-batch, CCR can induce accumulation of the non-preferred substrate, *e.g.* xylose in a dual xylose and glucose fermentation (Kim, Block and Mills 2010). A way to deal with this problem is to avoid CCR and create a non-diauxic xylose and glucose fermenting generalist (Kim *et al.* 2015) or to design xylose- and glucose-specialist species and performing fermentation with this synthetic consortium (Verhoeven *et al.* 2018). The ecological significance of CCR and observed microbial diversity in a mixed-substrate SBR environment fed with xylose and glucose can be used to design novel microbial-based processes using defined mixtures of pure cultures.

Using enrichment culturing with a mixture of xylose and glucose in a CSTR and SBR environment, we aimed to elucidate here the impact of mixed-substrate conditions on the microbial diversity and fermentative niche establishment in both environments. This was facilitated by comparing our results to previously published results for similar enrichment cultures with fermenting xylose or glucose in CSTR or SBR environments, inoculated with the same bovine rumen and also operated at pH 8, a temperature of 30°C and hydraulic retention time (HRT) of 8 h (Rombouts *et al.* 2019). Furthermore, we aim to evaluate the ecological significance of CCR using our enrichment culturing approach.

## Material and Methods

All enrichment procedures and analytical methods are described in detail in Rombouts *et al.* (2019). The main adaptations for the mixed-substrate experiments are given hereafter.

### Fermentative enrichment culturing

The enrichment procedure was executed as described in Rombouts *et al.* (2019), with the adaptation that 2 g $L^{-1}$ of xylose and 2 g $L^{-1}$ of glucose were fed as a mixture instead of 4 g $L^{-1}$ of one of the individual substrates, resulting in a similar COD influent concentration as in the single-substrate enrichments. The same cow rumen inoculum was used and seeded in the same way in the CSTR and SBR. The reactors were operated at 30°C±0.1, pH of 8.0±0.1 and a HRT of 8 h. The reactors were continuously stirred at 300 rpm and the solid retention time (SRT) is the same as the HRT applied. Steady state was assumed if during a period of at least 5 days no significant variation in the concentrations of fermentation products was observed.

### Analytical methods and cycle analysis

The concentrations of the residual glucose and xylose substrates and of the VFAs; formate to valerate), lactate, succinate, and ethanol substrates were analysed using high performance liquid chromatograph (HPLC) as described in Rombouts et al. (2019). Quantification was accurate in the range of 100-0.5 mM. For high butyrate concentrations above 1 mmol $L^{-1}$, samples were analysed using gas chromatography (GC) for butyrate and ethanol overlap in the refractive index (RI) spectrum and butyrate can be quantified from the ultraviolet (UV) spectrum, as described in Rombouts et al. 2019. The off-gases were monitored on-line for $H_2$ and $CO_2$ using a spectrophotometric method as described in Rombouts *et al.* (2019) and were accurately quantified in the range from 0.1-5%

Biomass concentration was measured using a standard method which relies on centrifugation to separate the cells from the medium, drying to obtain total suspended solids (TSS) and burning at 550°C to obtain volatile suspended solids (VSS) (APHA, 1998). This analysis was coupled to an optical density (OD) measurement at 660 nm to establish a correlation. OD values were used to calculate the biomass concentration during the batch experiments.

To characterise the kinetics of the cultures in SBR mode, one full cycle was sampled, and metabolite and biomass concentrations were measured in parallel to $H_2$ and $CO_2$ in the off-gas. In the CSTR, a batch test was conducted by removing 1 L of reactor broth and replacing it by 1 L of medium to finally obtain a concentration of 1 g $L^{-1}$ of xylose and 1 g $L^{-1}$ of glucose together with a stoichiometric amount of other nutrients. Sampling and off-gas analysis were carried out as in the SBRs over 5 h.

To characterise the mixed substrate uptake of the single substrate limited SBR enrichments, these enrichments were re-inoculated with 10 mL effluent from the xylose or glucose limited SBR enrichments obtained previously (Rombouts *et al.* 2019).Effluent frozen with 10% glycerol at -80°C was used to re-inoculate a SBR either on xylose or glucose using the previously described cultivation methods. These SBRs were operated for one week on either xylose or glucose, reaching steady state. Then, a batch cycle was characterized using a mixture of 1 g $L^{-1}$ of xylose and 1 g $L^{-1}$ of glucose.

**Microbial community analysis**

Genomic DNA was extracted from 2-mL samples of reactor suspension and the bacterial community compositions analysed as described in Rombouts *et al.* (2019). Analysis of V3-V4 16S rRNA gene-based amplicon sequencing was executed as described in Rombouts *et al.* (2019) to get an overview of the predominant populations selected in the enrichments over time. Cloning and sequencing of full-length 16S rRNA genes was conducted following Rombouts *et al.* (2019) to obtain species-level information, picking 38 clones for the CTSR

and 24 for the SBR enrichment. Primers used are listed in table S1. Amplicon sequencing data is available at NCBI under SRR8718538-SRR8718547 and full 16S clone sequences are available under MK185473-MK185614

Cell fixation and fluorescence *in situ* hybridisation (FISH) were carried out as described by Rombouts et al. (2019). Staining with 4′,6-diamidino-2-phenylindole (DAPI) was used to map all microbial cells. Cell surface area quantification was carried out using the Quantimet Interactive Programming System (QUIPS) feature of the Leica QWin V3 software (Leica, Germany).

**Mathematical modelling of the batch tests**

Mathematical modelling of the batch tests was carried out as described in Rombouts *et al.* (2019) using a simplified Herbert-Pirt equation for growth, neglecting maintenance:

$$\mu = Y_{xs} \cdot q_s \qquad (3)$$

Monod kinetics were used (equation 1) to describe the growth rate as a function of the substrate concentration at a $K_s$ value of 0.1 mmol $L^{-1}$ of either xylose or glucose. The model than estimated the buiomass and substrate values using the method described in Rombouts *et al.* (2019). A separate maximum biomass-specific rates of substrate consumption ($q_s^{max}$) were fitted for xylose and glucose in one batch test. The yields of biomass formation on substrates ($Y_{x,s}$) were fixed on glucose or xylose using the biomass yield obtained for the xylose or glucose SBR or the biomass yield obtained from the cycle measurement performed with the xylose or glucose CSTR from Rombouts *et al.* (2019).

**COD and carbon balances**

At steady state, carbon and chemical oxygen demand (COD) balances were set up using the method described in Rombouts *et al.* (2019) and the elemental matrix given in supplementary information of Rombouts *et al.* (2019). NADH and acetyl-CoA yields were set

up by multiplying the values in supplementary table  Rombouts *et al.* (2019) with the yield on glucose and xylose. A biomass composition of $C_1H_{1.8}O_{0.5}N_{0.2}$ was used (Roels 1983).

## Results

### Fermentations in SBR and CSTR enrichment cultures result in different product spectra

The two enrichment cultures operated with a mixture of xylose and glucose in SBR and CSTR mode showed a different fermentation product spectrum (Figure 1). The SBR enrichment initially produced predominantly acetate, ethanol and propionate (data not shown). When the steady state was reached, the SBR enrichment shifted to a product spectrum dominated by acetate and ethanol. The CSTR enrichment developed within 20 SRTs to a stable fermentation pattern producing primarily ethanol, acetate and butyrate (Figure 1). Mass and electron balances were almost closed with carbon and COD recovered to acceptable amounts (Table 1), indicating that all relevant fermentation products were identified.

### Xylose and glucose were taken up simultaneously, while xylose uptake was slower than glucose uptake

A cycle analysis or batch experiment was performed to estimate the $q_s^{max}$ and $\mu^{max}$ values of the enrichment cultures. Xylose and glucose were both instantly taken up by the enrichment cultures (Figure 2), indicating no carbon catabolite repression of glucose on xylose uptake in either culture. The xylose uptake rate was 2.7 and 1.7 times slower than glucose uptake rate in the SBR and CSTR enrichment culture, respectively. Both xylose and glucose uptake rates were higher in the SBR than CSTR enrichment culture (Table 2), with the summed $q_s^{max}$ values being 2.3 times higher for the SBR than for the CSTR culture. Noteworthy is the fact that the mixed-substrate CSTR enrichment culture displayed a combined $\mu^{max}$ only 31% above the applied dilution rate of 0.11 $h^{-1}$.

**Feeding a mixture of xylose and glucose led to one dominant microbial species in both CSTR and SBR enrichments**

According to dynamics of operational taxonomic units (OTUs) revealed by V3-V4 16S rRNA gene amplicon sequencing (Figure 3), the sequencing reads from the mixed-substrate CSTR were dominated by four populations affiliating with the genus *Citrobacter*, the family of *Enterobacteriaceae*, the family of *Lachnospiraceae*, and the genus *Clostridium*. All four populations stabilised after 20 SRTs, after an initial predominance of *Raoultella* and *Citrobacter* populations during the initial batch phase after which the reactor was switched into CSTR mode.

The sequencing reads of the mixed-substrate SBR were dominated by *Citrobacter* and *Enterobacteriaceae*. The same *Lachnospiraceae* genus as detected in the CSTR corresponded initially to 28% of the reads, stabilising at 13-15% later. Initially *Dysgonomonas* were present in significant amounts (11%, respectively, at 16 SRTs), decreasing to less than 2% at 38 SRTs of the reads. The fractions of other microbial groups in the SBR reads remained quite high at the end of the enrichment (31-35%) being composed of mostly of *Proteobacteria*, *Firmicutes*, *Actinobacteria* and *Bacteriodetes*.

The clone library of full-length 16S rRNA gene sequences established at the end of the enrichment was efficient to identify the dominant phylotypes with a species-level resolution (Figure 4). The amplicon sequencing results were reflected by the sequenced clone library. The predominance of *Citrobacter freundii*, *Clostridium intestinale* and two uncultivated *Lachnospiraceae* species gave a similar distribution in the CSTR enrichment (Figure 4). The composition of OTUs of the mixed-substrate SBR was also confirmed, with a predominance of *Citrobacter freundii*, and 8% fraction of the full 16S rRNA gene sequences corresponding to *Raoultella ornithinolytica*. An amount of 24 clones was picked for this library, which did not result in enough resolution to also identify the *Lachnospiraceae* population or species from the others fraction.

The FISH analysis revealed that the mixed-substrate SBR enrichment was dominated by *Enterobacteriaceae*, with 75% of the cell surface area showing fluorescence of the Ent183 probe (Table 3). A side population of *Lachnospiraceae* was also detected (8%). No cells hybridised with the *Clostridium*-targeting Chis150 probe. A significant fraction of 17% of microbial populations of the SBR enrichment remained unresolved by FISH. The CSTR enrichment was dominated by *Clostridium* (91%) with a side population of *Enterobacteriaceae* (11%) and a minor fraction of *Lachnospiraceae* (1%) (Table 3). Thus, the SBR enrichment was dominated by *Enterobacteriaceae* species and the CSTR enrichment to an even higher extend by *Clostridium* species. There is a clear discrepancy between the FISH observations and the DNA sequencing based observations, which will be discussed below.

## Discussion

### Mixed-substrate enrichment led to a similar spectrum of fermentation products as single-substrate enrichments

In this study we observed enrichment cultures on a mixture of glucose and xylose cultivated in the same way as previous enrichment cultures on the individual substrates (Rombouts *et al.* 2019). A comparison was made between a CSTR regime (always substrate limited uptake rates) and SBR regime (maximal substrate uptake rates). The product spectrum obtained when enriching a microbial community on a mixture of xylose and glucose was similar to the summation of the product spectra obtained on the single substrates (Figure S1) using the same inoculum and enrichment procedure. The formate and $H_2/CO_2$ ratio was different between the mixed-substrate SBR and the single-substrate SBRs summed up. The reason for this difference is not known, but the $k_La$ is likely excluded. The $k_La$ is the mass transfer coefficient and influences the transfer of liquid to gas phase. If this term changes under similar hydrogen production rates, a different hydrogen partial pressure is obtained, which potentially can affect the ratio of formate and hydrogen as the Gibbs energy change of the equilibrium between formate and hydrogen is assumed to be a constant value (Temudo, Kleerebezem

and van Loosdrecht 2007). We observed previously that different gas flow rates did not affect the formate and hydrogen ratio (Rombouts *et al.* 2019).

The mixed-substrate CSTR was producing more butyrate and less acetate and ethanol than the sum of the individual product spectra would suggest, though the spectrum is similar. Feeding a mixture of xylose and glucose to a CSTR fermentative community enriched on xylose has previously yielded to a similar observation: the product spectrum of a mixed-substrate enrichment has been similar, but not exactly the same to the theoretical summed product spectrum of a single-substrate enrichment (Temudo *et al.* 2009).

**Pathway analysis of the enrichments reveals pentose phosphate pathway (PPP) for xylose fermentation and no homoacetogenesis and electron bifurcation**

When comparing the products derived from acetyl-CoA and the formate and hydrogen yields (Table 1), it can be concluded that in both enrichment cultures acetate, ethanol, and butyrate were produced with a direct stoichiometric coupling with hydrogen or formate, through the decarboxylation of pyruvate to acetyl-CoA (Temudo, Kleerebezem and van Loosdrecht 2007; Rombouts *et al.* 2019). The NADH balance showed that slightly more NADH was consumed than produced in both enrichments (Table 1). This can be corrected by assuming a net NADH neutral production of succinate through both the reductive and oxidative pathways, equal to -0.04 and -0.02 mol $Cmol^{-1}$ for the SBR and CSTR cultures, respectively.

The PPP was assumed active in both enrichments since acetate and ethanol were produced in equimolar amounts and no excess of acetyl-CoA derivates over formate and hydrogen was detected (Table 1). The PKP produces directly one acetate and shuttles three carbon into glycolysis, leading to less production of formate and hydrogen and more acetate than ethanol. Furthermore, the nearly closing NADH balance and the equimolar amounts of acetyl-CoA derivates and formate and hydrogen indicates that homoacetogenesis and electron bifurcation did not play a significant role in these enrichments, as proposed by Regueira *et al.* (2018).

**Microbial community analysis showed a difference in biomass quantification between FISH and 16S-based methodologies**

In the mixed-substrate CSTR the 16S rRNA amplicon sequencing and the full 16S clone library suggested that a *Clostridium*, *Citrobacter* and *Lachnospiraceae* population where present in equal amounts in the community (Figure 3 and 4). The FISH analysis however showed a dominance of *Clostridium* (Table 3 and Figure S3B). This difference can arise from a DNA extraction bias or PCR amplification bias (Brooks *et al.* 2015) or from the fact the *Clostridium* cells contain an equal amount of 16S DNA but are 5-10 times bigger than the *Citrobacter* and *Lachnospiraceae* cells, as visible using light microscopy (Figure S5).

The amount of biomass (or biovolume), rather than the cell number, is representative for the share in substrate turn-over in a microbial community. This amount of biomass is assessed by FISH where a quantification is made based on cell-surface area. Recently in other studies a similar discrepancy between biovolume and cell numbers due to differences in cell size have been reported (Saccà 2016; Domaizon *et al.* 2017; Rubio-Rincón *et al.* 2019) A “full cycle rRNA analysis” of a microbial community structure, as proposed by Amann, Ludwig and Schleifer (1995) is needed to get a quantitative view of a microbial community structure. Such as cycle consists of first identifying the dominant taxa in a given sample (*e.g.* 16S rRNA amplicon sequencing), and then using a quantitative tool like FISH to estimate the fractions of these taxa in a sample.

**The CSTR enrichment resulted in a dominance of a generalist species**

We originally hypothesised that a CSTR enrichment based on a mixture of equivalent substrates would lead to the dominance of a generalist species over specialist species. The microbial community analysis showed that the mixed-substrate CSTR enrichment was dominated by a *Clostridium* population (Table 3, Figure S3) mainly composed of *Clostridium intestinale* (Figure 4). This species was also dominating a glucose-limited CSTR enrichment (Rombouts *et al.* 2019) and can be linked to butyrate production, as the CSTR produces a significant amount of butyrate where the SBR does not. Apparently, this species is

competitive in both a sole glucose-limited CSTR environment and a dual xylose- and glucose-limited CSTR environment.

To dominate under dual limitations, *C. intestinale* needs to have a high affinity uptake system for glucose and for xylose expressed. For glucose, the phosphotransferase system (PTS) and methyl-galactoside transport system ATP-binding protein (Mgl) have both been described as high-affinity transporters (Jahreis *et al.* 2008). For xylose, the xylose ABC (ATP-binding cassette) transport operon (XylFGH) is known as a high-affinity uptake system (Sumiya *et al.* 1995). The closest related strain of which a genome is available is *C. intestinale* strain JCM 7506 (NCBI:txid1121320), also known as strain DSM 6191 (99% identity). This strain contains all three subunits of the PTS system in its genome and the xylose-binding protein XylF, enabling it to competitively take up glucose and xylose in a continuous substrate limited environment, leading to its dominance in a mixed-substrate environment (Figure 5). XylG and XylH are not found in its genome, but other ABC type ATP-binding proteins and membrane spanning proteins, found in the genome could fulfil these roles.

Previously, Temudo *et al.* (2008) have characterised the effect of switching from feeding xylose or glycerol to feeding an equal amount of xylose and glucose or glycerol and glucose. They have observed that a similar amount or even less bands were observed in the molecular fingerprint of the bacterial community obtained after one week or 21 SRTs of enrichment by denaturing gradient gel electrophoresis. This indicated that adding a mixture of limiting substrates does not necessarily lead to more microbial diversity, confirming our observation in the mixed-substrate CSTR, where a *C. intestinale* was the dominating the microbial community in terms of biovolume.

**SBR enrichment leads to dominance of a dual xylose- and glucose-fermenting species**

In the mixed substrate SBR, a dominance of *Enterobacteriaceae* with a side population of *Lachnospiraceae* affiliates was observed (Table 3, Figure S4). Previously we have reported the dominance (>90%) of *Enterobacteriaceae* affiliates on SBRs limited on either glucose or xylose (Rombouts *et al.* 2019). The significant side population of *Lachnospiraceae* present in the mixed-substrate SBR enrichment might have been caused by rather long cleaning intervals of wall biofilm. In this study the SBR was cleaned every 3-9 SRTs versus 3 SRTs in Rombouts *et al. (*2019) (Table S6). The biofilm formed was presumably adding microbial diversity to the community in the form of *Lachnospiraceae*. We expect that a 3 SRT cleaning schedule would have led to an enrichment dominated completely (>90%) by *Enterobacteriaceae*.

Well-studied microorganisms such as *E. coli* display CCR in batch (Deutscher 2008). Therefore, we hypothesised that a diauxic generalist species fermenting first glucose and then xylose would coexist with a specialist for xylose. We find *Citrobacter freundii* as the dominant *Enterobacteriaceae* in the mixed-substrate SBR enrichment, when assuming DNA extraction, copy number and PCR biases to be similar in this family (Figure 4) and a non-diauxic uptake of xylose and glucose (Figure 2). This species was also dominant in the xylose SBR enrichment (Rombouts et al. 2019), and showed a non-diauxic uptake for xylose when subjected to a cycle with xylose and glucose (Figure S2B).

*Citrobacter freundii* strains are known to ferment both xylose and glucose (Farmer *et al.* 1985). The $q_s^{max}$ of the sole xylose enrichment was 2.28±0.10 $Cmol_S\ Cmol_X^{-1}\ h^{-1}$ (Rombouts *et al.* 2019), while the mixed substrate SBR enrichment showed a combined $q_s^{max}$ of 2.80±0.04 $Cmol_s\ Cmol_x^{-1}\ h^{-1}$, which is similar to the value of the xylose SBR subjected to glucose and xylose, 2.68±0.04 $Cmol_s\ Cmol_x^{-1}\ h^{-1}$. The dominant *C. freundii* species outcompetes xylose specialists by attaining a higher overall $q_s^{max}$ on xylose and glucose, and therefore a higher $q_s^{max}$ than what is achievable on xylose as sole carbon source. It has been shown that *E. coli* can achieve a higher catabolic flux when taking up glucose compared to xylose (Gonzalez, Long and Antoniewicz 2017). This can underlie why dual xylose glucose

383 uptake in our study led to higher overall flux. Apparently, a xylose specialist or a CCR-type
384 generalist are outcompeted by a non-diauxic dual fermenting generalist.

385 XylE is a xylose symporter which is associated with high rate and low affinity (Sumiya *et al.*
386 1995) which makes this transporter likely to be expressed at high growth conditions with
387 substrate in excess, *e.g.* batch cultivation. Outer membrane protein C (OmpC) and OmpF
388 allow glucose to diffuse into the cell at high substrate concentration (>0.2 mM) while lambda
389 receptor protein B (LamB) is induced under lower glucose concentrations (Luo, Zhang and
390 Wu 2014). The dominant strain in the mixed SBR enrichment is *C. freundii* strain P10159
391 (CP012554.1, 100% identity), which was also the dominant strain in the xylose SBR
392 enrichment (Rombouts *et al.* 2019). This strain contains the genes to express XylE, OmpC
393 and LamB, which argues for its competitive uptake of both substrates. Xylose uptake is
394 inhibited through a cAMP mediated pathway (Luo, Zhang and Wu 2014). Since this species
395 exhibited no CCR in our enrichments, it would be of interest to identify how this species
396 regulates its glucose and xylose uptake.

397 A niche is present for a glucose specialist, fermenting glucose at a $\mu^{max}$ and $q_s^{max}$ higher than
398 that of the generalist. A minor fraction of *Raoultella ornithinolytica* was detected (Figure 4),
399 which was also detected in a minor amount in the glucose SBR enrichment (Rombouts *et al.*
400 2019). Potentially, this species takes up glucose at a higher rate than the generalist,
401 enabling them to coexist (Figure 6). Since the generalist grows on both xylose and glucose,
402 this species is assumed to dominate the enrichment, which was reflected by the clone library
403 (Figure 4).

404 It has been shown that repeated batch cultivation at 60°C (5 SRTs) leads to the presence of
405 three populations for glucose, one for xylose, and four for a mixture of glucose and xylose
406 (Hniman, O-Thong and Prasertsan 2011). Since this study only characterised the microbial
407 community after 5 SRTs, it is quite possible that the microbial diversity would have
408 decreased for the all three enrichments. Microbial population dynamics can lead to a

relatively long time for communities to stabilize which is visible in the mixed substrate SBR (Figure 4). A *Dysgonomonas* population emerged in the reads at 7 SRTs and then became a minor fraction at 38 SRTs, indicating some microbial interaction to take place in this timespan which causes a more diverse community structure.

Here we conclude that enriching in a CSTR using mixed substrates lead to a dominant generalist species, confirming our hypothesis and the chemostat theory that describes the competitive advantage of a generalist in a chemostat. In the SBR, a generalist species was fermenting the xylose and glucose without carbon catabolite repression, which was not expected, postulating that contrary to many pure culture studies xylose and glucose are taken up in the environment by generalists without CCR. In dual substrate uptake, xylose fermentation is slower than glucose fermentation and product spectra of mixture of xylose and glucose are similar to product spectra from solely xylose or glucose. Microbiologists designing an industrial mixed substrate fermentation of a lignocellulosic residue containing glucose and xylose should consider that a non-diauxic generalist is competitive in such an environment.

**Acknowledgements** (funding, people)

The authors thank Cor Ras and Max Zomerdijk for technical assistance in analytics, Ben Abbas for help with the clone libraries and sequencing, Lars Puiman for his help in improving the FISH hybridisation for Gram+ microorganisms, and Stef van Hateren for constructing the Leica V3 software to quantify FISH targeted cell surfaces, all at the Delft University of Technology. This work was supported by the Soenhgen Institute for Anaerobic Microbiology (SIAM), SIAM gravitation grant, the Netherlands Organization for Scientific Research (024.002.002). The authors declare that they have no conflict of interest.

## References


Amann RI, Ludwig W, Schleifer KH. Phylogenetic identification and in situ detection of individual microbial cells without cultivation. *Microbiol Rev* 1995;**59**:143–69.

Anwar Z, Gulfraz M, Irshad M. Agro-industrial lignocellulosic biomass a key to unlock the future bio-energy: A brief review. *J Radiat Res Appl Sci* 2014;**7**:163–73.

APHA. *Standard Methods for the Examination of Water and Wastewater*. 20th ed. Washington D.C.: American Public Health Association, 1998.

Beijerinck M. Anhaufungsversuche mit Ureumbakterien. *Cent f Bakteriol* 1901;**7**:33–61.

Bell WH. Bacterial utilization of algal extracellular products. 1. The kinetic approach. *Limnol Oceanogr* 1980;**25**:1007–20.

Brooks JP, Edwards DJ, Harwich MD *et al.* The truth about metagenomics: Quantifying and counteracting bias in 16S rRNA studies Ecological and evolutionary microbiology. *BMC Microbiol* 2015;**15**:1–14.

Deutscher J. The mechanisms of carbon catabolite repression in bacteria. *Curr Opin Microbiol* 2008;**11**:87–93.

Dionisi D, Anderson J a., Aulenta F *et al.* The potential of microbial processes for lignocellulosic biomass conversion to ethanol: a review. *J Chem Technol Biotechnol* 2015;**90**:366–83.

Domaizon I, Rimet F, Jacquet S *et al.* Avoiding quantification bias in metabarcoding: Application of a cell biovolume correction factor in diatom molecular biomonitoring. *Methods Ecol Evol* 2017;**9**:1060–9.

Fang HHP, Liu H. Effect of pH on hydrogen production from glucose by a mixed culture. *Bioresour Technol* 2002;**82**:87–93.

Farmer JJ, Davis BR, Hickman-Brenner FW *et al.* Biochemical identification of new species and biogroups of Enterobacteriaceae isolated from clinical specimens. *J Clin Microbiol* 1985;**21**:46–76.

Gonzalez JE, Long CP, Antoniewicz MR. Comprehensive analysis of glucose and xylose metabolism in Escherichia coli under aerobic and anaerobic conditions by13C metabolic flux analysis. *Metab Eng* 2017;**39**:9–18.

Görke B, Stülke J. Carbon catabolite repression in bacteria: many ways to make the most out of nutrients. *Nat Rev Microbiol* 2008;**6**:613.

Gottschal JC, de Vries S, Kuenen JG. Competition between the facultatively chemolithotrophic Thiobacillus A2, an obligately chemolithotrophic Thiobacillus and a heterotrophic spirillum for inorganic and organic substrates. *Arch Microbiol* 1979;**121**:241–9.

Guo XM, Trably E, Latrille E *et al.* Hydrogen production from agricultural waste by dark fermentation: A review. *Int J Hydrogen Energy* 2010;**35**:10660–73.

Hansen, Hubbell SP. Single-nutrient microbial competition: qualitative agreement between experimental and theoretically forecast outcomes. *Science (80- )* 1980;**207**:1491 LP – 1493.

Hniman A, O-Thong S, Prasertsan P. Developing a thermophilic hydrogen-producing microbial consortia from geothermal spring for efficient utilization of xylose and glucose mixed substrates and oil palm trunk hydrolysate. *Int J Hydrogen Energy* 2011;**36**:8785–93.

Jahreis K, Pimentel-Schmitt EF, Brückner R *et al.* Ins and outs of glucose transport systems in eubacteria. *FEMS Microbiol Rev* 2008;**32**:891–907.

Jiang Y, Marang L, Kleerebezem R *et al.* Polyhydroxybutyrate production from lactate using a mixed microbial culture. *Biotechnol Bioeng* 2011;**108**:2022–35.

Johnson K, Jiang Y, Kleerebezem R *et al.* Enrichment of a Mixed Bacterial Culture with a High Polyhydroxyalkanoate Storage Capacity. *Biomacromolecules* 2009;**10**:670–6.

Kim JH, Block DE, Mills DA. Simultaneous consumption of pentose and hexose sugars: An optimal microbial phenotype for efficient fermentation of lignocellulosic biomass. *Appl Microbiol Biotechnol* 2010;**88**:1077–85.

Kim SM, Choi BY, Ryu YS *et al.* Simultaneous utilization of glucose and xylose via novel mechanisms in engineered Escherichia coli. *Metab Eng* 2015;**30**:141–8.

Kleerebezem R, Joosse B, Rozendal R *et al.* Anaerobic digestion without biogas? *Rev Environ Sci Biotechnol* 2015;**14**:787–801.

Kleerebezem R, van Loosdrecht MC. Mixed culture biotechnology for bioenergy production. *Curr Opin Biotechnol* 2007;**18**:207–12.

Kuenen JG. The Role of Specialists and Generalists in Microbial Population Interactions. *Foundations of Biochemical Engineering*. AMERICAN CHEMICAL SOCIETY, 1983, 10–229.

Kuenen JG. *Continuous Cultures (Chemostats)☆*. Elsevier Inc., 2015.

Lendenmann U, Egli T. Kinetic models for the growth of Escherichia coli with mixtures of sugars under carbon-limited conditions. *Biotechnol Bioeng* 1998;**59**:99–107.

Luo Y, Zhang T, Wu H. The transport and mediation mechanisms of the common sugars in Escherichia coli. *Biotechnol Adv* 2014;**32**:905–19.

Meyer H-P, Minas W, Schmidhalter D. Industrial-scale fermentation. *Ind Biotechnol Prod Process* 2017:1–53.

Noike T, Endo G, Chang J-E *et al.* Characteristics of carbohydrate degradation and the rate-limiting step in anaerobic digestion. *Biotechnol Bioeng* 1985;**27**:1482–9.

Postma E, Kuiper A, Tomasouw WF *et al.* Competition for glucose between the yeasts Saccharomyces cerevisiae and Candida utilis. *Appl Environ Microbiol* 1989;**55**:3214–20.

Rafrafi Y, Trably E, Hamelin J *et al.* Sub-dominant bacteria as keystone species in microbial communities producing bio-hydrogen. *Int J Hydrogen Energy* 2013;**38**:4975–85.

Regueira A, González-Cabaleiro R, Ofiţeru ID *et al.* Electron bifurcation mechanism and homoacetogenesis explain products yields in mixed culture anaerobic fermentations. *Water Res* 2018:5–13.

Roels JA. *Energetics and Kinetics in Biotechnology.* Amsterdam: Elsevier B.V., 1983.

Rombouts JL, Mos G, Weissbrodt DG *et al.* Diversity and metabolism of xylose and glucose fermenting microbial communities in sequencing batch or continuous culturing. *FEMS Microbiol Ecol* 2019;**95**.

Rubio-Rincón FJ, Welles L, Lopez-Vazquez CM *et al.* Effect of Lactate on the Microbial Community and Process Performance of an EBPR System. *Front Microbiol* 2019;**10**:1–11.

523 Saccà A. A simple yet accurate method for the estimation of the biovolume of
524 planktonic microorganisms. *PLoS One* 2016;**11**:1–17.

525 Steinbusch KJJ, Hamelers HVM, Plugge CM *et al.* Biological formation of caproate
526 and caprylate from acetate: Fuel and chemical production from low grade
527 biomass. *Energy Environ Sci* 2011;**4**:216–24.

528 Sumiya M, O Davis E, C Packman L *et al.* Molecular genetics of a receptor protein
529 for D-xylose, encoded by the gene xylF in Escherichia coli. *Receptors Channels*
530 1995;**3**:117–28.

531 Temudo MF, Kleerebezem R, van Loosdrecht M. Influence of the pH on (open)
532 mixed culture fermentation of glucose: a chemostat study. *Biotechnol Bioeng*
533 2007;**98**:69–79.

534 Temudo MF, Mato T, Kleerebezem R *et al.* Xylose anaerobic conversion by open-
535 mixed cultures. *Appl Microbiol Biotechnol* 2009;**82**:231–9.

536 Temudo MF, Muyzer G, Kleerebezem R *et al.* Diversity of microbial communities in
537 open mixed culture fermentations: Impact of the pH and carbon source. *Appl*
538 *Microbiol Biotechnol* 2008;**80**:1121–30.

539 Verhoeven MD, de Valk SC, Daran J-MG *et al.* Fermentation of glucose-xylose-
540 arabinose mixtures by a synthetic consortium of single-sugar-fermenting
541 Saccharomyces cerevisiae strains. *FEMS Yeast Res* 2018;**18**:1–12.

542

543

## Tables

Table 1: Carbon and COD balances, product yields and biomass yields in the glucose and xylose fed SBR and CSTR enrichment cultures. Acetyl-CoA derivates and formate and hydrogen yields and NADH yields were calculated on the basis of our previously published biochemical network (Rombouts *et al.* 2019). Yields are given per C-mol substrate.

| | Carbon [%] | COD [%] | Acetyl-CoA derivates [mol $Cmol^{-1}$] | Formate + $H_2$ [mol $Cmol^{-1}$] | NADH [mol $Cmol^{-1}$] | $Y_{x,s}$ [Cmol $Cmol^{-1}$] |
|---|---|---|---|---|---|---|
| SBR | 99 ± 2 | 99 ± 1 | 0.25 ± 0.01 | 0.25 ± 0.02 | -0.07 ± 0.01 | 0.15 ± 0.00 |
| CSTR | 97 ± 5 | 96 ± 2 | 0.25 ± 0.01 | 0.24 ± 0.01 | -0.04 ± 0.00 | 0.15 ± 0.00 |

Table 2: Modelled $q_s^{max}$ and $\mu^{max}$ for glucose or xylose during the cycle analysis for the mixed-substrate SBR enrichment and CSTR enrichment (measured data in Figure 2). The $\sigma_{qsmax}$ was calculated using error propagation and the covariance of the $C_s$ and $C_{x,0}$ measurement, while $\sigma_{\mu max}$ was calculated using error propagation and the covariance of the $C_x$ and $C_{x,0}$ measurement. Biomass yields used to estimate the growth rate are taken from the enrichments on solely xylose or glucose as growth substrate (Rombouts *et al.* 2019).

| | | Mixed-substrate SBR | Mixed-substrate CSTR |
|---|---|---|---|
| Glucose | $q_s^{max}$ [$Cmol_s$ $Cmol_x^{-1}$ $h^{-1}$] | 2.01± 0.03 | 0.78 ± 0.01 |
| | $\mu^{max}$ [$h^{-1}$] | 0.26 ± 0.01 | 0.11 ± 0.01 |
| Xylose | $q_s^{max}$ [$Cmol_s$ $Cmol_x^{-1}$ $h^{-1}$] | 0.79 ± 0.01 | 0.46 ± 0.01 |
| | $\mu^{max}$ [$h^{-1}$] | 0.09 ± 0.01 | 0.06 ± 0.01 |
| Summed | $q_s^{max}$ [$Cmol_s$ $Cmol_x^{-1}$ $h^{-1}$] | 2.80 ± 0.04 | 1.24 ± 0.02 |
| | $\mu^{max}$ [$h^{-1}$] | 0.36 ± 0.04 | 0.17 ± 0.03 |

Table 3: Microbial composition analysis based on FISH quantification (average of three different measurements) of dominant populations in the mixed-substrate SBR and CSTR. Percentages denote relative abundances calculated from the target-probe surface compared to EUB338 surface. Unidentified populations were calculated as the remaining percentage after summing up the relative abundances of the known populations in the first three columns. The last column shows the amount of surface probed by EUB338 compared to DAPI. Samples used were taken at 86 SRTs for CSTR and 37 SRTs for SBR. ND = not detected.

| | **Chis150** *vs.* EUB338 [%] | **Lac435** *vs.* EUB338 [%] | **Ent183** *vs.* EUB338 [%] | **Unidentified** *vs.* EUB338 [%] | **EUB338** *vs.* DAPI [%] |
|---|---|---|---|---|---|
| Mixed-substrate SBR | ND | 8±6 | 75±8 | 17 | 103±24 |
| Mixed-substrate CSTR | 91±2 | 1±1 | 11±6 | -2 | 102±24 |

## Figures

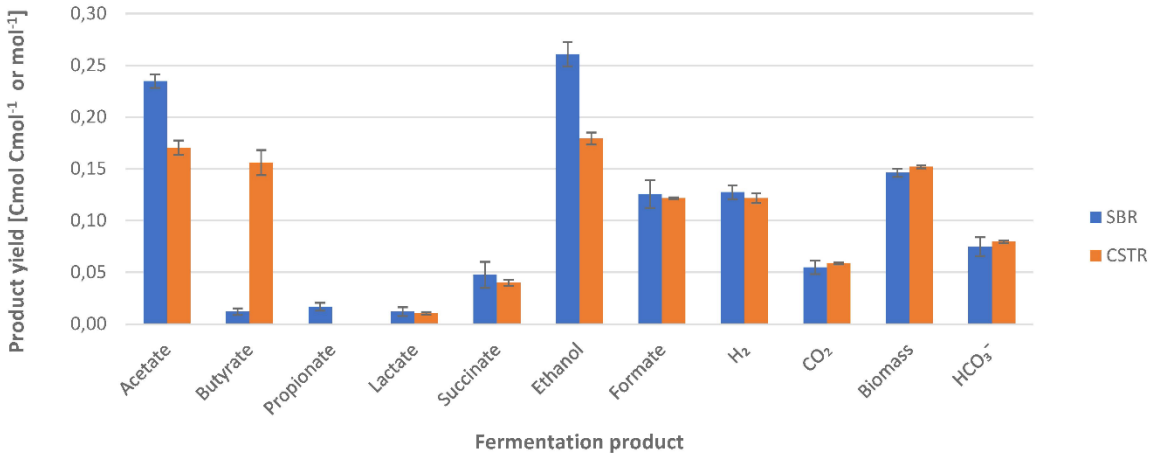


Figure 1: Steady state fermentation product spectra of glucose and xylose fed SBR and CSTR in Cmol or mol product per Cmol substrate on the basis of three measurements in time.

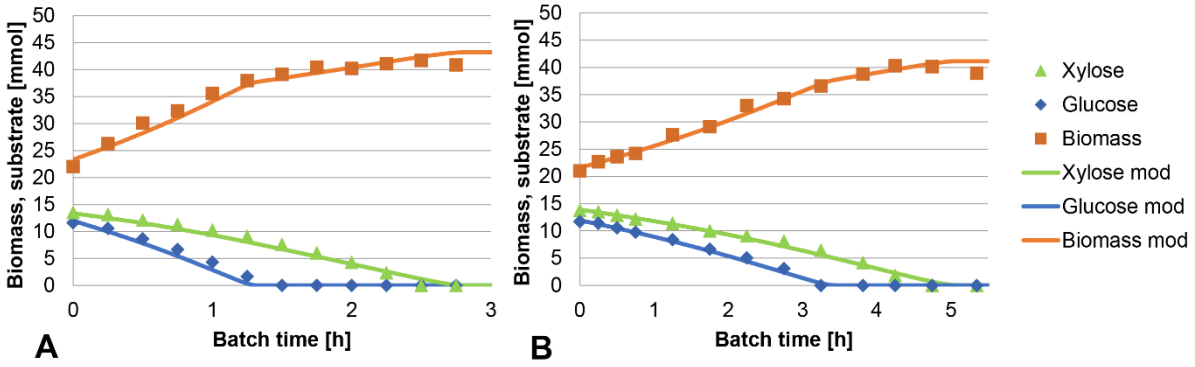


Figure 2: Measured and modelled glucose, xylose and biomass concentrations during the cycle analysis in the SBR (A) and CSTR (B) enrichment cultures. Both modelled results showed a $R^2 > 0.99$.

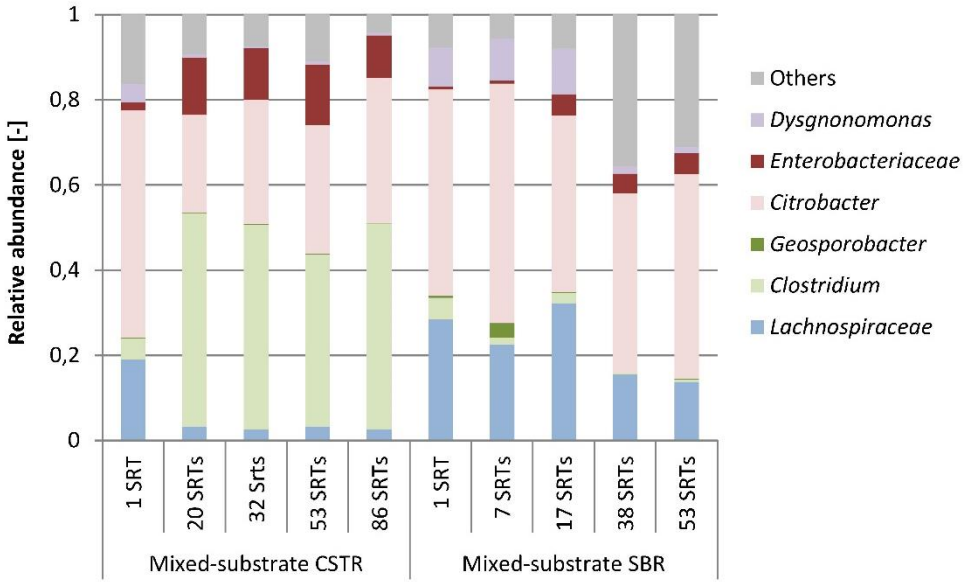


577

578 Figure 3: Relative abundance of genera obtained from V3-V4 16S rRNA gene amplicon
579 sequencing read counts. Genera of the *Enterobacteriaceae* family are shown in red colours
580 and genera of the *Clostridiaceae* are shown in green colours. OTUs accounting for less than
581 3% of the reads were bundled into “others” (grey).

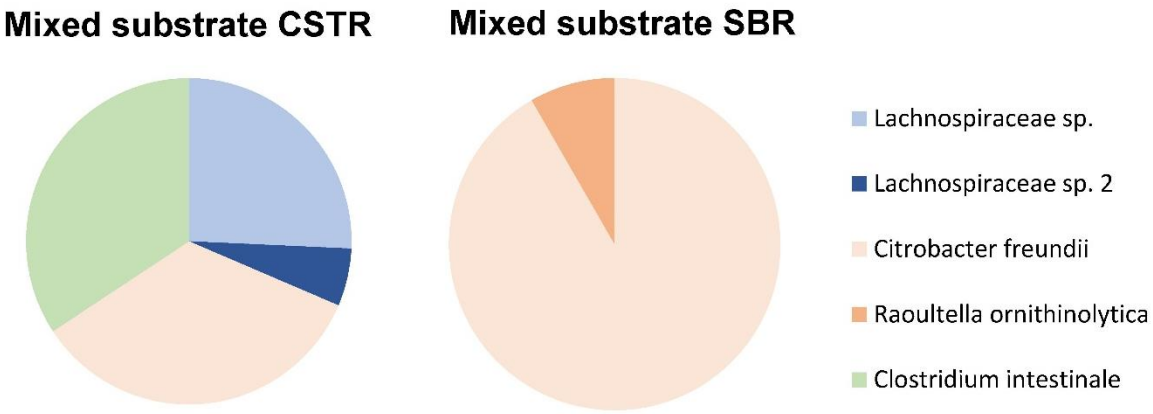


582

583 Figure 4: Microbial composition as estimated by cloning and sequencing of full-length 16S
584 rRNA gene sequences of the bacterial populations in the mixed-substrate CSTR and SBR

enrichments. *Lachnospiraceae* species are denoted in blue colours, *Enterobacteriaceae* species in red colours and *Clostridiaceae* species in green colours. Samples used are 86 SRTs for CSTR and 53 SRTs for SBR.

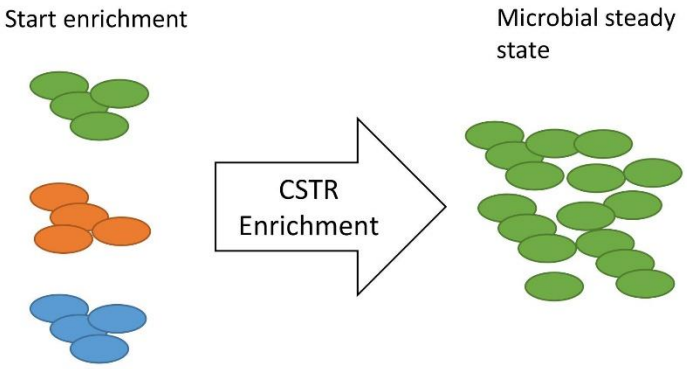


| Species | Xylose uptake XylFGH | Glucose uptake PTS II ABC |
|---|---|---|
| Generalist | + | + |
| Glucose specialist | - | + |
| Xylose specialist | + | - |

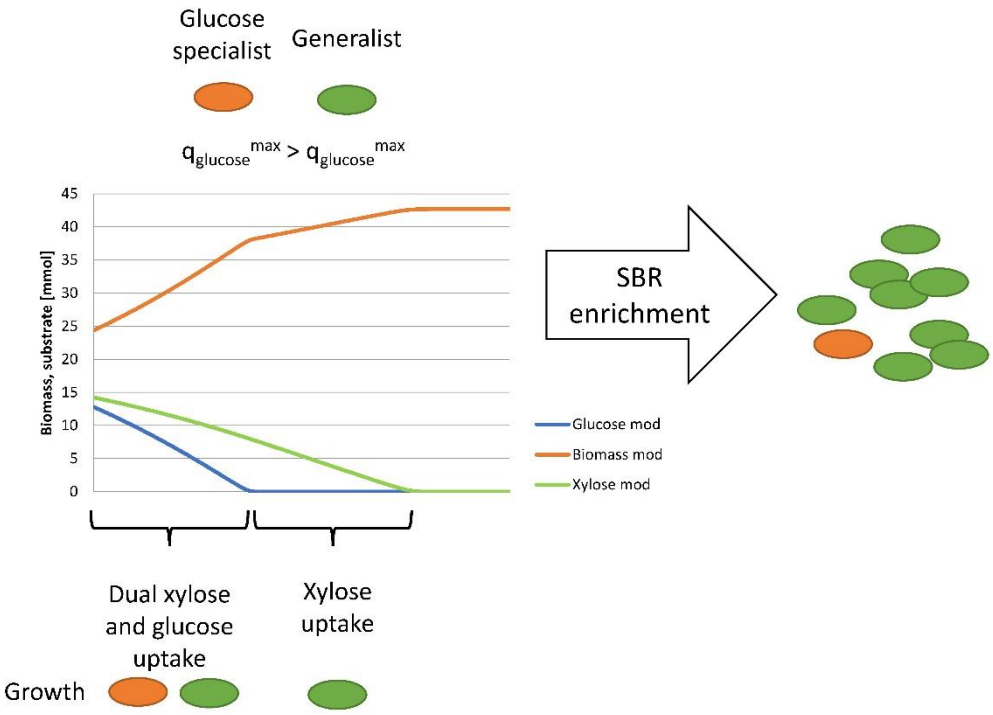


591

592 Figure 6: Competition between a high-rate glucose specialist (orange) and a dual xylose-
593 and glucose-fermenting generalist (green). In the first phase, glucose is taken up by both
594 species, while in the second phase xylose is only taken up the generalist.

595

## Supplementary Information

Table S1: Primers used in this study

| Primer | Primer Sequence (5'- 3') | Reference |
|---|---|---|
| 341f | CCT AYG GGR BGC ASC AG | (Muyzer, de Waal and Uitterlinden 1993) (Caporaso *et al.* 2011) |
| 806r | GGA CTAC NNG GGT ATC TAA T | (Muyzer, de Waal and Uitterlinden 1993) (Caporaso *et al.* 2011) |
| GM3f | AGA GTT TGA TCM TGG CTC AG | (Weisburg *et al.* 1991) |
| GM4r | GGT TAC CTT GTT ACG ACT T | (Weisburg *et al.* 1991) |
| M13f | GTA AAA CGA CGG CCA G | (Invitrogen 2014) |
| M13r | CAG GAA ACA GCT ATG AC | (Invitrogen 2014) |

Table S2: FISH probes used in this study with the formamide concentration used during hybridisation

| FISH Probe | Sequence 5'- 3' | Specificity | Formamide [%] | Reference |
|---|---|---|---|---|
| EUB338 Cy5 | GCT GCC TCC CGT AGG AGT | Bacteria | 20-25 | (Amann *et al.* 1990) |
| ENT183 Cy3 | CTC TTT GGT CTT GCG ACG | *Enterobacteriaceae* family | 20 | (Friedrich *et al.* 2003) |
| Chis150 Cy3 | TCT TCC CTG CTG ATA GA | *Clostridium* genus | 25 | (Franks *et al.* 1998) |
| Lac435 Cy3 | TTA TGC GGT ATT AAT CTY CCT TT | *Lachnospiraceae* family | 25 | (Kong *et al.* 2010) |

## References

Amann RI, Binder BJ, Olson RJ et al. Combination of 16S rRNA-targeted oligonucleotide probes with flow cytometry for analyzing mixed microbial populations. Appl Environ Microbiol 1990;56:1919–25.

Caporaso JG, Lauber CL, Walters WA et al. Global patterns of 16S rRNA diversity at a depth of millions of sequences per sample. Proc Natl Acad Sci U S A 2011;108 Suppl 1:4516–22.

610 Franks AH, Harmsen HJM, Raangs GC et al. Variations of bacterial populations in
611 human feces measured by fluorescent in situ hybridization with group-specific 16S rRNA-
612 targeted oligonucleotide probes. Appl Environ Microbiol 1998;64:3336–45.

613 Friedrich U, Van Langenhove H, Altendorf K et al. Microbial community and
614 physicochemical analysis of an industrial waste gas biofilter and design of 16S rRNA-
615 targeting oligonucleotide probes. Environ Microbiol 2003;5:183–201.

616 Invitrogen. TOPO TA Cloning Kit for Sequencing. Carlsbad, 2014.

617 Kong Y, He M, McAlister T et al. Quantitative Fluorescence In Situ Hybridization of
618 Microbial Communities in the Rumens of Cattle Fed Different Diets. Appl Environ Microbiol
619 2010;76:6933–8.

620 Muyzer G, de Waal EC, Uitterlinden AG. Profiling of complex microbial populations
621 by denaturing gradient gel electrophoresis analysis of polymerase chain reaction-amplified
622 genes coding for 16S rRNA. Appl Environ Microbiol 1993;59:695–700.

623 Weisburg WG, Barns SM, Pelletier DA et al. 16S ribosomal DNA amplification for
624 phylogenetic study. J Bacteriol 1991;173:697–703.

625

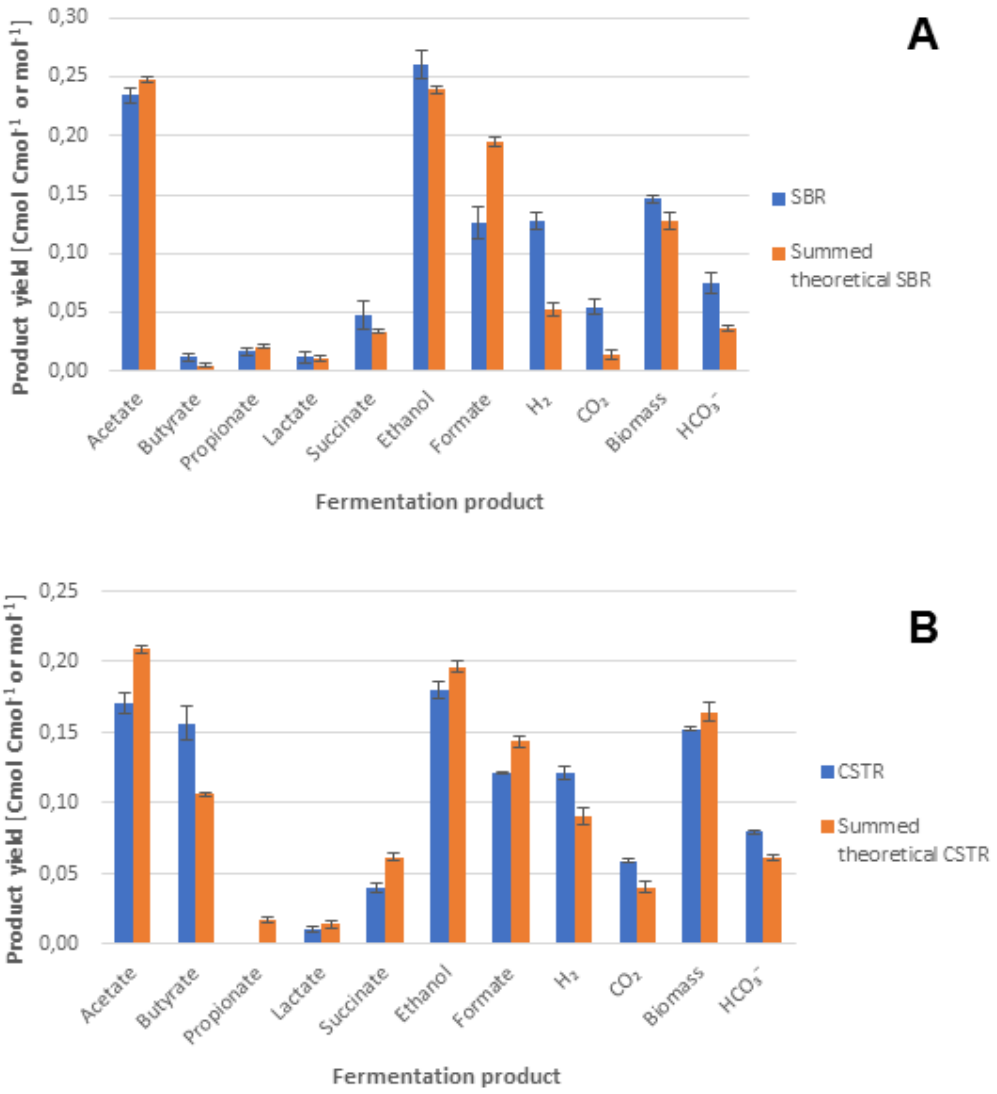


626

627 Figure S1: The obtained product spectrum for the mixed-substrate SBR (A) and CSTR (B)
628 compared to the theoretical summed SBR (A) and CSTR (B) product spectrum based on the
629 yields obtained for the single substrate enrichments (Rombouts *et al.* 2019) and using 50%
630 of the xylose and glucose obtained yields, respectively.

631

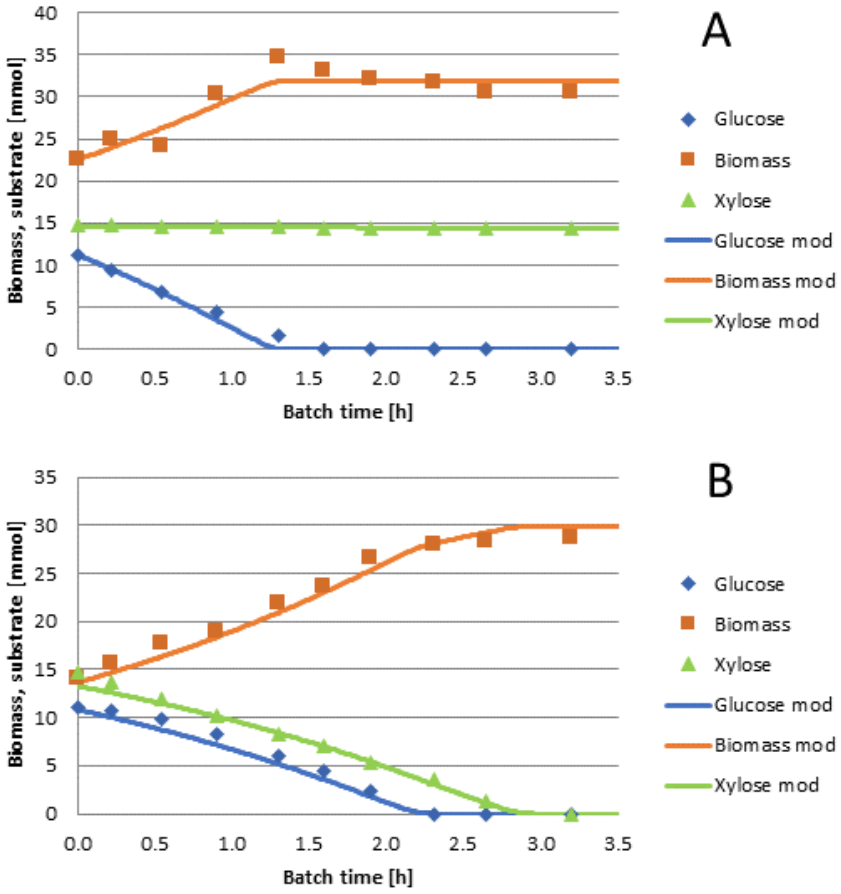


632

633 Figure S2: Simultaneous uptake of xylose and glucose during a cycle analysis performed in
634 the glucose-fed SBR enrichment culture (A) and the xylose-fed SBR enrichment culture (B)
635 enriched previously (Rombouts *et al.* 2019). Biomass yields on xylose and glucose were
636 fixed and obtained from previous reported biomass yields on either xylose or glucose
637 (Rombouts *et al.* 2019). $R^2$ values are 0.84 and 0.99 for A and B respectively.

638

Table S3: Modelled $q_s^{max}$ and $\mu^{max}$ for glucose or xylose during the cycle analysis with both substrates for the glucose-fed SBR enrichment culture and the xylose-fed SBR enrichment culture enriched previously (Rombouts *et al.* 2019). Covariance of the biomass and xylose and glucose measurements were used to calculate the covariance of the rates.

| | | Glucose-fed SBR | Xylose-fed SBR |
|---|---|---|---|
| Glucose | $q_s^{max}$ [$Cmol_s\ Cmol_x^{-1}\ h^{-1}$] | 2.10 ± 0.03 | 1.56 ± 0.02 |
| | $\mu^{max}$ [$h^{-1}$] | 0.28 ± 0.00 | 0.21 ± 0.00 |
| Xylose | $q_s^{max}$ [$Cmol_s\ Cmol_x^{-1}\ h^{-1}$] | 0.00 ± 0.00 | 1.12 ± 0.02 |
| | $\mu^{max}$ [$h^{-1}$] | 0.00 ± 0.00 | 0.13 ± 0.00 |
| Summed | $q_s^{max}$ [$Cmol_s\ Cmol_x^{-1}\ h^{-1}$] | 2.10 ± 0.03 | 2.68 ± 0.04 |
| | $\mu^{max}$ [$h^{-1}$] | 0.28 ± 0.00 | 0.34 ± 0.01 |

644 Table S4: Result using BLASTn of the reference OTU sequences obtained using V3-V4 16S

645 rRNA gene amplicon sequencing

| Accession number | Identity | E value | Query cover | Total score | Maximum score | Closest cultivated relative | Label figure | Colour |
|---|---|---|---|---|---|---|---|---|
| MG812314.1 | 100% | 0 | 100% | 793 | 793 | Citrobacter freundii strain ER1 16S ribosomal RNA gene, partial sequence | *Citrobacter* | |
| MH681450.1 | 100% | 0 | 100% | 793 | 793 | Raoultella ornithinolytica strain BE3.4 16S ribosomal RNA gene, partial sequence | *Raoultella* | |
| MF737172.1 | 100% | 0 | 100% | 793 | 793 | Klebsiella oxytoca strain B2006 16S ribosomal RNA gene, partial sequence | *Klebsiella* | |
| AJ630276.1 | 99% | 0 | 100% | 767 | 767 | Dysgonomonas gadei partial 16S rRNA gene, clone MFC-EB6 | *Dysgonomonas* | |
| LT855382.1 | 99% | 0 | 100% | 719 | 719 | Lachnospiraceae bacterium Marseille-P3773 partial 16S rRNA gene, strain Marseille-P3773 | *Lachnospiraceae* | |
| CP017269.1 | 100% | 0 | 100% | 8196 | 747 | Geosporobacter ferrireducens strain IRF9, complete genome | *Geosporobacter* | |
| LC037210.1 | 100% | 0 | 100% | 747 | 747 | Clostridium intestinale gene for 16S ribosomal RNA, partial sequence, strain: JCM 7506 | *Clostridium* | |

646

647 Table S5: Result using BLASTn on the representative sequences per OTU obtained after
648 sequencing of the clone library of full-length 16S rRNA genes. Relative abundance per OTU
649 are given at the bottom of the table.

| Accession | Ident | E value | Query cover | Total score | Max score | Description - closest related cultivated species | Fractions | Colour |
|---|---|---|---|---|---|---|---|---|
| MF953294.1 | 96% | 0.0 | 99% | 2259 | 2259 | Lachnotalea glycerini strain DLD10 16S ribosomal RNA gene, partial sequence | *Lachnospiraceae sp.* | |
| MF574095.1 | 92% | 0.0 | 96% | 1875 | 1875 | Lachnotalea glycerini strain CCRI-19302 16S ribosomal RNA gene, partial sequence | *Lachnospiraceae sp. 2* | |
| CP012554.1 | 100% | 0.0 | 100% | 21094 | 2638 | Citrobacter freundii strain P10159, complete genome | *Citrobacter freundii* | |
| CP026056.1 | 99% | 0.0 | 100% | 20612 | 2610 | Citrobacter freundii strain FDAARGOS_73 chromosome, complete genome | *Citrobacter freundii* | |
| CP026056.1 | 99% | 0.0 | 100% | 20172 | 2562 | Citrobacter freundii strain FDAARGOS_73 chromosome, complete genome | *Citrobacter freundii* | |
| KF358448.1 | 99% | 0.0 | 100% | 2612 | 2612 | Raoultella ornithinolytica strain FMC41 16S ribosomal RNA gene, partial sequence | *Raoultella ornithinolytica* | |
| AY781385.1 | 99% | 0.0 | 100% | 2588 | 2588 | Clostridium intestinale 16S ribosomal RNA gene, complete sequence | *Clostridium intestinale* | |
| **CSTR** | | | | | | | | |
| 0.26 | | | | | | | | |
| 0.058 | | | | | | | | |
| 0.17 | | | | | | | | |
| 0.14 | | | | | | | | |
| 0.029 | | | | | | | | |
| 0 | | | | | | | | |
| 0.34 | | | | | | | | |
| **SBR** | | | | | | | | |
| 0 | | | | | | | | |
| 0 | | | | | | | | |
| 0.88 | | | | | | | | |
| 0.04 | | | | | | | | |
| 0 | | | | | | | | |
| 0.08 | | | | | | | | |
| 0 | | | | | | | | |

650

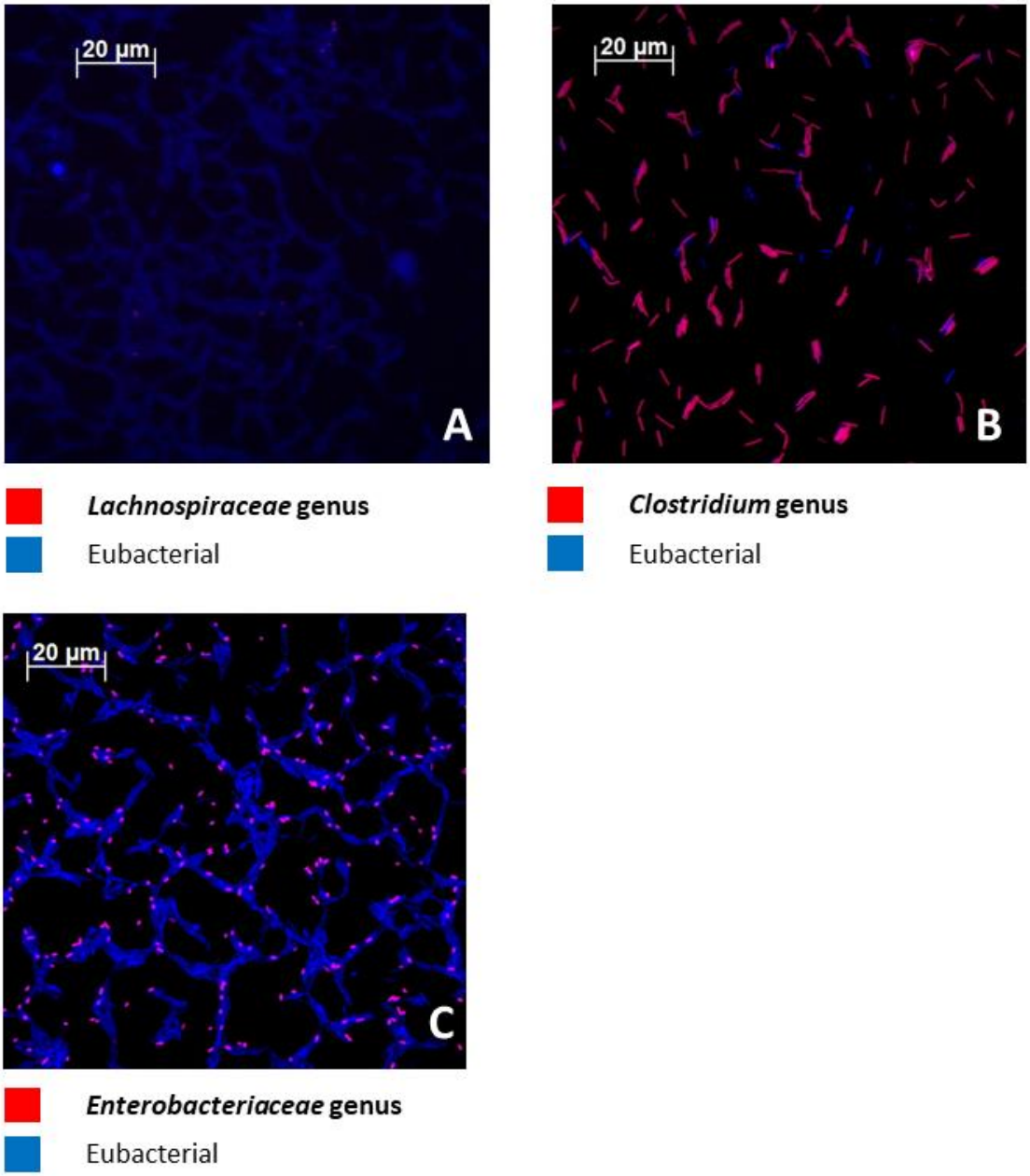


651

652 Figure S3: Typical result obtained by FISH analysis of the mixed-substrate CSTR
653 enrichment culture after 86 SRTs using the EUB338 mix oligonucleotide probes to target all
654 eubacterial species, Lac435 to target *Lachnospiraceae*, Chis150 to target *Clostridium* and
655 Ent183 to target *Enterobacteriaceae*

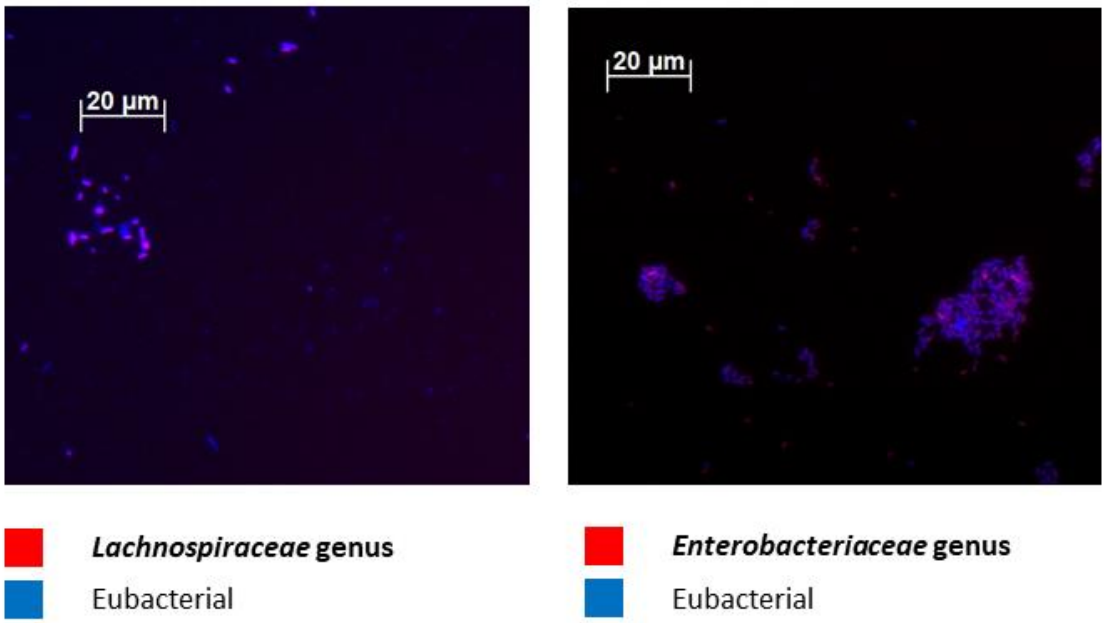


656

657 Figure S4: Typical result obtained by FISH analysis of the mixed-substrate SBR enrichment
658 culture after 37 SRTs using the EUB338 mix probes to target all eubacterial species, Lac435
659 probe to target *Lachnospiraceae*, and Ent183 to target *Enterobacteriaceae*

660

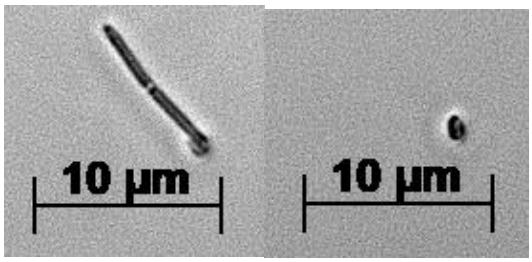


661

662 Figure S5: Phase contrast image using bright field microscopy of a *Clostridium* cell (left) and
663 a *Citrobacter* or *Lachnospiraceae* cell (right). The image was digitally sharpened using the
664 Zeiss Axio software

665

666

667 Table S6: Intervals of cleaning of the wall biofilm developing in the mixed-substrate SBR

| Date | SRTs | SRTs between cleaning |
|---|---|---|
| **23-5-2017** | 1 | 0 |
| **24-5-2017** | 2 | 1 |
| **26-5-2017** | 4 | 2 |
| **29-5-2017** | 7 | 3 |
| **31-5-2017** | 11 | 4 |
| **2-6-2017** | 17 | 6 |
| **4-6-2017** | 23 | 6 |
| **6-6-2017** | 29 | 6 |
| **8-6-2017** | 35 | 6 |
| **9-6-2017** | 38 | 3 |
| **12-6-2017** | 47 | 9 |
| **13-6-2017** | 50 | 3 |
| **14-6-2017** | 53 | 3 |

668

669

670